

Development of A Flux-Switching Permanent Magnet Motor for Hybrid Electric Vehicles

Zhongze Wu, Wei Hua, Ming Cheng

School of Electrical Engineering, Southeast University, China

E-mail : huawei1978@seu.edu.cn

Abstract —In this paper, an improved structure of a 3-phase 12-stator-slot/10-rotor-pole flux-switching permanent magnet motor based on the original topology is proposed by comparison of several solutions for a practical 10kW integral starter/generator system in hybrid electric vehicles, in which the magnets and armature windings can be easily fixed. The design and static characteristics including phase flux-linkage, back-EMF waveforms, cogging torque as well as electromagnetic torque of each structure are evaluated based on 2-D finite element analysis (FEA). Compared with an interior PM motor in Honda Civic, the results indicated that the developed FSPM motor exhibits preferable performance.

I. INTRODUCTION

The comparative results between a flux-switching permanent magnet (FSPM) motor and a traditional surface-mounted PM (SPM) motor having the same specifications reveal that FSPM motor exhibits larger airgap flux-density, higher torque per copper loss, but also higher torque ripple due to cogging torque [1]. However, as shown in Fig. 1(a), both the magnets and armature windings of an original 3-phase 12-stator-slot/10-rotor-pole FSPM motor are susceptible to moving in radial direction due to vibration in a running vehicle. Hence, an improved structure based on the original FSPM motor structure is proposed by comparison of several solutions for practical application. To address this problem, in this paper several solutions are proposed and compared by evaluation of the electromagnetic performance based on 2-D finite element analysis (FEA). Finally, compared with a prototyped interior PM motor in Honda Civic, a developed FSPM motor exhibits preferable performance with the nearly same dimensions.

II. DEVELOPED TOPOLOGIES

Based on the original structure of magnet (Fig. 2(a)), a couple of rectangular and deltoid grooves are introduced in Fig. 2(b) and (c), respectively. Moreover, a developed stator tooth with tips is proposed as shown in Fig. 2(e). The basic design dimensions are illustrated in Fig. 3 and listed in Table I.

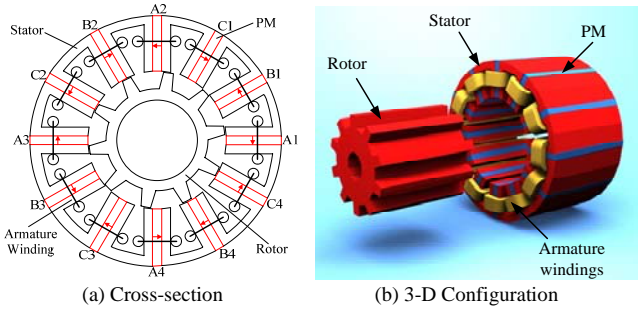


Fig. 1. The structure of a 12/10-pole FSPM motor.

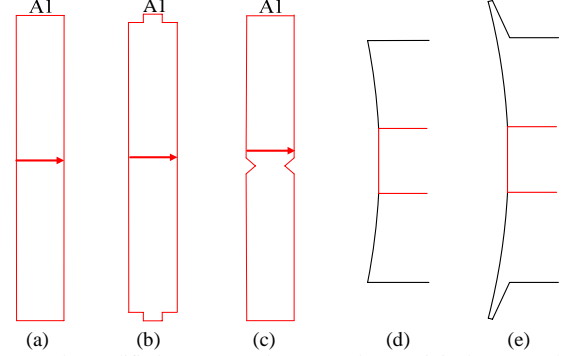


Fig. 2. The modified magnets and stator teeth. (a) original magnet, (b) magnet with rectangular grooves, (c) magnet with deltoid grooves, (d) origin stator tooth, (e) modified stator teeth with pole tips.

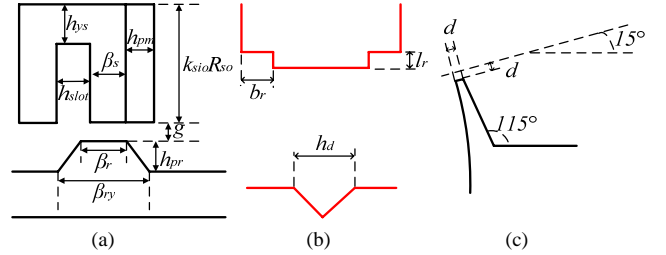


Fig. 3. Design dimensions of the original structure and modified structures. (a) original topology (b) magnets with grooves (c) stator tooth with pole tips

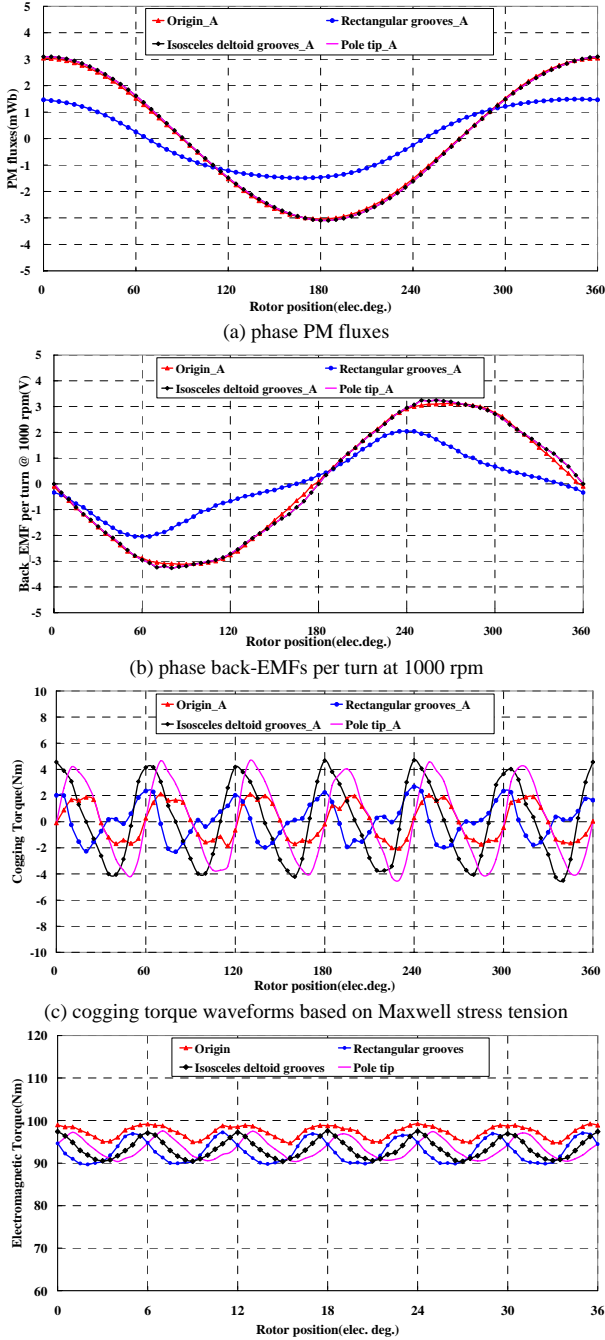
TABLE I
DESIGN SPECIFICATIONS OF THE ORIGINAL AND MODIFIED STRUCTURES

Items	FSPM motor
Base Speed (rpm)	1000
Stator outer radius (mm), R_{so}	240
Stack length (mm), l_a	40
Stator split ratio, k_{sio}	0.6
Rotor inner diameter (mm), R_{ri}	40
Stator slot number, P_s	12
Rotor pole number, P_r	10
Airgap length (mm), g	0.9
Stator pole arc (degree), β_s	8.25
Stator slot arc (degree), h_{slot}	7.5
magnet arc (degree), h_{pm}	6
Rotor pole arc (degree), β_r	10.5
Rotor pole-yoke arc (degree), β_{ry}	21
Rectangular groove breadth (mm), b_r	1
Rectangular groove length (mm), l_r	1.5
Deltoid groove hypotenuse (mm), h_d	0.5
Pole tip breadth (mm), d	0.5

III. ELECTROMAGNETIC PERFORMANCE

The predicted PM flux-linkage per turn, back-EMF at 1000 rpm of phase A, the cogging waveforms and electromagnetic torque of four structures based on Maxwell stress tension are showed in Fig. 4. As can be seen in Fig. 4, in the case of introducing rectangular grooves in the top and bottom of the

magnet, both the waveforms of the phase PM flux and back-EMF are far away from sinusoidal due to the leakage as shown in Fig. 5, whereas the peak value of cogging torque is only slightly larger than the original one. However, in the other two cases of introducing deltoid grooves in the middle of magnet and pole-tips in stator tooth, the distortions of flux and back-EMF can be negligible, whereas the peak values of cogging torque are both significant larger than the original structure. Hence, finally the deltoid grooves and pole tips are added into the original structure as a developed topology (Fig. 6(a)).



(d) electromagnetic torque based on Maxwell stress tension ($J_s=5.17\text{A/mm}^2$)
Fig. 4. The static characteristics of the FSPM motor with different topologies.

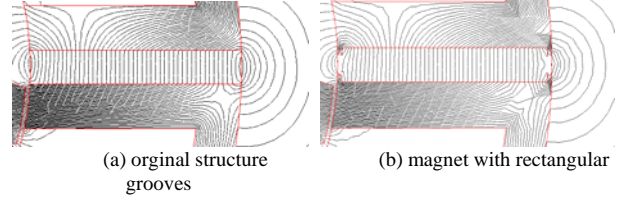


Fig. 5. Open-circuit field distributions of the FSPM motor at $\theta_r=0^\circ$ positions.

IV. COMPARISON OF FSPM AND IPM MOTORS

Fig. 6 compares the open-circuit flux distributions of the developed FSPM motor and a prototyped IPM motor in Honda Civic. It should be noted that the IPM motor has a slightly larger stator outer diameter (253.7mm). However, from Fig. 7 it can be found that the FSPM motor exhibits a larger torque under the same armature current density and stack length, indicating the preferable prospect of application.

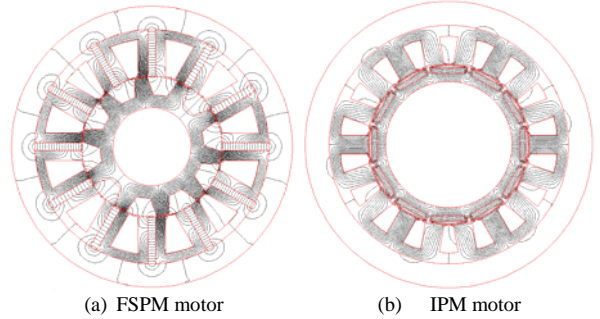


Fig. 6. Open-circuit field distributions of the FSPM motor and Honda civic motor (the stator out diameter is 253.7mm).

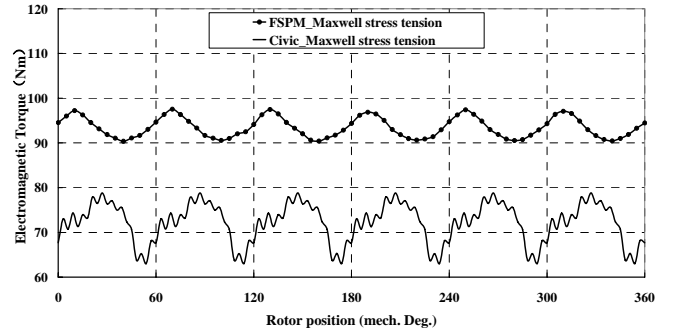


Fig. 7. Electromagnetic torques of two motors with the same current ($J_s=5.17\text{A/mm}^2$).

ACKNOWLEDGMENTS

This work was supported by National Natural Science Foundation of China (50807007), the Specialized Research Fund for the Doctoral Program of Higher Education of China (200802861038), the Fund Program of Southeast University for Excellent Youth Teachers, Southeast University Science Fund for Distinguished Young Scholars, Southeast University Key Science Research Fund, and a grant from the Key Technology R&D Program of Jiangsu Province, China (BE2009085).

REFERENCES

- [1] Wei Hua, Ming Cheng, Z.Q. Zhu. Comparison of electromagnetic performance of brushless motors having magnets in stator and rotor, Journal of Applied Physics, 2008, 103(7): 07F124.